Journal of Thermal Analysis and Calorimetry, Vol. 69 (2002) 717–725

THERMAL CHARACTERISTICS IN A NANOMETER SCALE

I. Hatta[*]

Faculty of General Education, Fukui University of Technology, Fukui 910-8505, Japan

Abstract

As examples of studies on thermal characteristics of materials with a nanometer scale two topics are discussed. One is heat capacity and thermal conductivity of small materials at low temperatures. It based upon the recent findings that heat capacity depends on the limited number of the phonon modes in low angular frequency region and the distinct characteristic is the appearance of quantized thermal conductance in heat transfer through a narrow wire with hundreds nm. The other is the thermophysical properties at the ordinary interface. The disordered structure appearing in the interfacial region with a width of a few nm is discussed, which is comparable to the phonon mean free path, should be taken into account to reveal the characteristic thermal behavior at room temperature.

Keywords: heat capacity, interface, nanometer, nanotechnology, thermal conductivity, thermal diffusivity

Introduction

Recently, we are being able to control or manipulate atoms or molecules to organize mesoscale materials. The studies on thermal characteristics in such materials are challenging subjects. To consider the thermal characteristics, phonon or electron mean free path plays an important role, since it lies in a few tens nanometer at room temperature. Usually, it becomes long at low temperatures and therefore, the dimensions associated with the thermal characteristics depends on temperature. In this paper, some of topics for the thermal characteristics will be introduced. The attention will be focused on the thermal behavior: (1) at low temperatures, (2) in an interfacial region.

Heat capacity and thermal conductivity at low temperature

Heat capacity of low dimensional materials near 0 K

At low temperatures (low T), heat capacity of bulk materials can be explained mostly in terms of the Debye's heat capacity formula, that is, the heat capacity is proportional to T^3 since the phonon density of states (phonon DOS) is proportional to the square of acoustic

* E-mail: hatta@ccmails.fukui-ut.ac.jp

1418–2874/2002/ $ 5.00

Akadémiai Kiadó, Budapest
Kluwer Academic Publishers, Dordrecht

angular frequency ω^2. Generally by taking into account the phonon dispersion curves associated with the acoustic phonon blanches, we can obtain the phonon DOS. Then, we can derive the Debye's heat capacity formula. We know that in a one-dimensional material, the phonon DOS is constant against ω and therefore near 0 K the heat capacity is proportional to T; in a two-dimensional material the phonon DOS is linearly related to ω and therefore near 0 K the heat capacity is proportional to T^2.

Heat capacity and thermal conductivity of a single-wall carbon nanotube at low temperatures

A single-wall carbon nanotube is one of one-dimensional materials. Heat capacity of the bundle of tens to hundreds of single-wall carbon nanotubes with diameter of 1.25 nm has been measured from 2 to 300 K with a relaxation method [1]. Above 4 K, the behavior of a single-wall carbon nanotube reflecting one-dimensional character takes place and below 4 K, the heat capacity deviates from the behavior of a single-wall carbon nanotube. The latter is due to the three-dimensional character resulting from the lateral interaction between carbon nanotubes in the bundle.

Heat capacity of a small plate

Within the framework of the Debye's model, the phonon DOS of a plane-like material is linearly proportional to ω. However this is not the case in a small plate. The phonon DOS is modified at low frequencies significantly as shown schematically in Fig. 1, i.e., there is a cutoff frequency below which there is no mode owing to the limitation of the length of the sample and furthermore, the displacement out of plane should be taken into account. These affect the temperature dependence of the heat capacity. Let us consider a thermally isolated square plate of silicon nitride (4 μm×4 μm×60 nm). There are four phonon modes just above the cutoff frequency (the lowest energy bound): a dilatational mode, two flexural modes and a torsional mode. Far above the energy of these four modes the higher harmonics of these modes appear as shown in Fig. 1. Therefore, in the low temperature region the temperature dependence of the heat capacity reflects only the above four modes in which the angular frequencies are denoted by ω_1, ω_2, ω_3 and ω_4 ($\omega_1<\omega_2<\omega_3<\omega_4$). For the contribu-

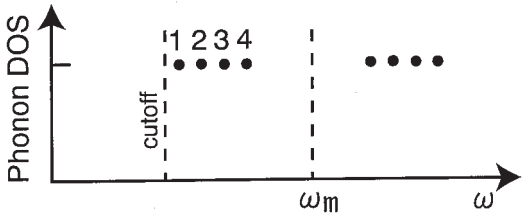

Fig. 1 Phonon density of states (phonon DOS) for a small square plate. Just above the cutoff angular frequency there are the four angular frequencies for one dilatational, two flexural and one torsional mode. ω_m lies at higher angular frequency than for these four modes and at lower frequency than for the higher harmonics of the four modes

tion of each mode to the heat capacity, we can apply the Einstein's heat capacity formula for *i*-th mode as

$$C_{\mathrm{Vi}}=k_{\mathrm{B}}\frac{\mathrm{e}^{\hbar\omega_{\mathrm{i}}/k_{\mathrm{B}}T}}{(\mathrm{e}^{\hbar\omega_{\mathrm{i}}/k_{\mathrm{B}}T}-1)^2}\left(\frac{\hbar\omega_{\mathrm{i}}}{k_{\mathrm{B}}T}\right)^2 \tag{1}$$

where k_{B} is the Boltzmann constant and $\hbar$ is the Planck constant divided by 2π. The total heat capacity for the four modes is given by

$$C_{\mathrm{v}}=\sum_{\mathrm{i}=1}^{4}C_{\mathrm{vi}}. \tag{2}$$

Assuming that the sound velocity of silicon nitride is about 10^4 m s^{-1}, $\hbar\omega_{\mathrm{i}}$ for the above frequency range is roughly estimated for the small plate with the area of 4×4 μm. From the relation of $\hbar\omega_{\mathrm{i}}\approx k_{\mathrm{B}}T_{\mathrm{vib}}$, it is derived that T_{vib} is about 0.05 K. In the temperature region of $T_{\mathrm{m}}>>T_{\mathrm{vib}}$, i.e., $\omega_{\mathrm{m}}>>\omega_{\mathrm{i}}$ where $\hbar\omega_{\mathrm{m}}\approx k_{\mathrm{B}}T_{\mathrm{m}}$, we obtain

$$C_{\mathrm{v}}\approx 4k_{\mathrm{B}} \tag{3}$$

It should be pointed out that the heat capacity is extremely small since it does not include the Avogadro's constant. The temperature T_{vib} becomes much higher if we can prepare an isolated sample with much smaller dimensions.

Quantized thermal conductance at low temperatures

The recent progress in the quantum effect of phonon thermal conductance will be introduced. The flow of the electrons through a narrow constriction between two large conductors leads theoretically to the quantum of electric conductance in units of $2e^2/h$ using the Landauer formulation of transport theory, where $\hbar$ is the Planck constant and e is the electric charge of an electron [2]. The quantized electric conductance steps have been observed in quantum wires [3, 4]. We can expect similar behavior in the phonon transport. Using also the Landauer formulation, it has been demonstrated theoretically that in a low temperature region dominated by ballistic phonon transport the phonon thermal conductance in one-dimensional wire is quantized [5]. The quantum of thermal conductance per a phonon mode, g_0, is given by [5]

$$g_0=\frac{\pi^2 k_{\mathrm{B}}T}{3h} \tag{4}$$

It should be pointed out that g_0 is devoid of any material parameters, such as the thermophysical properties. The reason why g_0 is proportional to T is due to the fact that at low temperatures the thermal conductivity is proportional to the heat capacity and furthermore the heat capacity in one-dimension is linear *vs*. T.

Schwab *et al*. [6] have measured the quantized thermal conductance. In their experiments, when a thermal gradient is applied along an electrically insulating wire, heat is carried from the hot to the cold reservoir by phonon modes within the wire. The hot phonon reservoir is composed of a square plate of silicon nitride

(4 μm×4 μm×60 nm), to which two thin-film gold transducers are placed. Heat is generated by one transducer and the temperature of the square plate is detected by another transducer. The isolated hot reservoir heated by the transducer is suspended by four phonon waveguides with the narrowest width less than 200 nm. The four phonon waveguides are coupled to the cold reservoir which constructs the frame of the whole mesoscopic system. Under such a setup, the experiments have been performed and the quantized thermal conductance has been observed [6]. In the above setup, the four phonon modes contribute the quantized thermal conductance at low temperatures and through the four phonon waveguides heat is carried. Therefore, the quantized thermal conductance at low temperatures is estimated to be $16g_0$ ($=g_0\times4\times4$). When the observed thermal conductance is divided by $16g_0$, the normalized thermal conductance exhibits unity below ca 0.8 K. This is evidence of the quantized thermal conductance. Above ca 0.8 K the normalized thermal conductance shows a cubic power behavior. This is due to the fact that in this temperature region the phonon mean free path becomes less than 0.9 μm and then, the three dimensional behavior appears as expected.

Interfacial region and phonon mean free path

Superlattice

Superlattice has been used for a variety of applications. From a viewpoint of basic science, since superlattice possesses a lot of interfaces, it is a useful material to study the thermophysical properties of the interface. So far many studies on the thermophysical properties of superlattices have been performed. In the present paper, I will focus my attention to the thermophysical properties of the interface which are measured along the direction normal to the interfaces. Let us consider Bi_2Te_3/Sb_2Te_3 superlattice grown on a silicon substrate by a laser ablation technique. The thickness of a single layer of Bi_2Te_3 was the same as that of Sb_2Te_3. The thickness of each single layer ranged from 3.4 to 60 nm. The number of a pair of Bi_2Te_3/Sb_2Te_3 layers lay in 160 and 13 in order. The total thickness of the superlattice was about 1 μm. The upper surface of the superlattice was heated by a modulated laser beam. Then, the ac temperature waves propagated normal to the surface by repeating the reflections and penetrations at the interfaces or the interfacial regions. Finally the ac temperature waves reach the boundary between the superlattice and the silicon substrate. The phase difference of the ac temperatures between the upper surface of the superlattice and the boundary of the superlattice and the substrate was measured as a function of frequency in the range from 0.5 to 5 MHz.

To analyze the results, we take into account two models [7]. In one model, there is a sharp interface between Bi_2Te_3 and Sb_2Te_3 layers as shown in Fig. 2A. In the other model, there is an interfacial region composed of a disordered structure as shown in Fig. 2B. It is surprising that in these models, the experimental results can be well explained likewise. Then, it is impossible to judge which model is the better only from the experiments. The analyzed results are as follows. In the former the interfacial thermal resistance is about $1.4\cdot10^{-8}$ K m^2 W^{-1} and in the latter the thickness of the in-

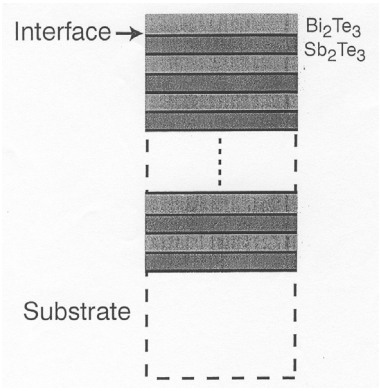

Fig. 2a Schematic view for Bi_2Te_3/Sb_2Te_3 superlattice on a substrate. Between Bi_2Te_3 and Sb_2Te_3 layers there is an interface

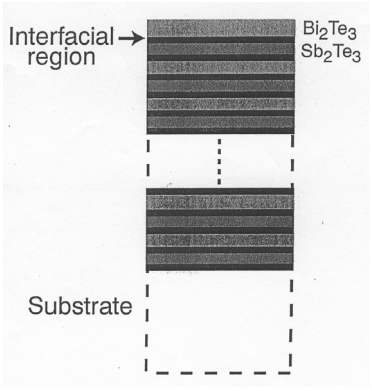

Fig. 2b Schematic view for Bi_2Te_3/Sb_2Te_3 superlattice on a substrate. Between Bi_2Te_3 and Sb_2Te_3 layers there is an interfacial region

terfacial region is about 1.5 nm under the assumption that its thermal conductivity is almost equal to that of the alloy $BiSbTe_3$, about 0.11 W K^{-1} m^{-1}.

At low temperatures, generally the phonon mean free path becomes long. Then, if there is disorder at an interface, the thickness is far smaller than the phonon mean free path and therefore, in the ballistic phonon transfer the interface behaves like a sharp boundary. Then, the interfacial thermal resistance due to the acoustic mismatch, the diffuse mismatch, etc. should be taken into account [8]. So far many experimental results have been analyzed in terms of the interfacial thermal resistance even at room temperature. However, at room temperature the phonon mean free path is no longer large enough and then, we cannot ignore the disordered interfacial region with a certain thickness, where the disorder due to the lattice distortion, the mixing of chemical compositions, etc. takes place. In fact, Swartz and Pohl [8] have pointed out that in the heat transfer across the ordinary interfaces near and above room temperature we have to pay attention to the disorder in the interfacial region.

To verify the disordered interfacial region, one of the useful methods is a distance variation method (an ac calorimetric method) [9]. Using the method, the thermophysical properties along the interfaces of the superlattice can be measured as a function of the layer thickness. In the superlattice of GaAs/AlAs, Yao [10] has measured the thermal diffusivity in a free-standing thin plate of the superlattice as a function of the layer thickness and made clear that the thermal diffusivity become small markedly with the decrease of the layer thickness. This fact indicates that the interfacial region between the neighboring layers has disorder character since without considering the disordered structure in the interfacial region we cannot explain the thickness dependence of the thermal diffusivity. His results have been reanalyzed by taking into account a disordered interfacial region with a certain thickness [11]. From the analysis, the thickness of the interfacial region is estimated to be about 4 nm by assuming that the thermal conductivity in the interfacial region is similar to that in the alloy of $Ga_{0.5}Al_{0.5}As$.

I should stress that to understand the thermophysical properties at the ordinary interface at room temperature it is important to take into account the contribution of its structure. At the ordinary interface appearing in nanotechnology, the structure of the interfacial region is more or less regarded as disorder and its thickness is about a few nm. Furthermore, the boundary around the interfacial region is not sharp, i.e., it accompanies with a certain structural relaxation. On the other hand, the phonon mean free path in the interfacial region seems to be cross to that in the alloy, i.e., it is about a few nm usually. Then, when heat transmits across the interfacial region, phonon scattering takes place within the interfacial region.

Comment on the interfacial thermal resistance measured by 3ω method

From a 3ω method the interfacial thermal resistance has been estimated at the interface between a thin film and a substrate. For a sample system in the 3ω method, a thin insulating film with the thickness of d is grown on the surface of the substrate as seen in the upper illustration of Fig. 3A and a metal film with fine width is deposited on the top of the thin film. The ac Joule heat with 2ω is generated at the metal film and the ac signal with 3ω is detected by the same metal film. Thus obtained thermal resistance R is given by

$$R=\frac{d}{\lambda}+R_{\mathrm{i}} \tag{5}$$

where λ is the thermal conductivity of the thin film and R_{i} is the interfacial thermal resistance due to the acoustic mismatch, etc. As shown in the lower graph of Fig. 3A, we can obtained λ from the slope of R *vs*. d and R_{i} from the intercept. In a SiO_2 film grown on a Si substrate, the measurements of the thermal resistance have been performed and the interfacial thermal resistances have been estimated [12, 13]. Thus obtained interfacial thermal resistance is about $2\cdot10^{-8}$ K m^2 W^{-1}. Kim *et al*. [13] have pointed out that in this measurement the interfacial thermal resistance includes the

contribution of the both thermal resistance between the thin film and the substrate and that between the thin film and the thin metal film.

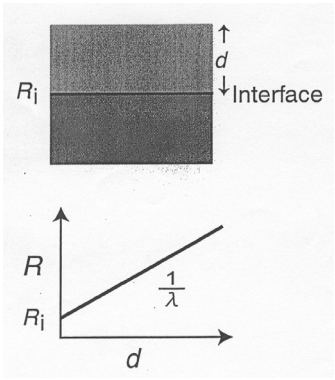

Fig. 3a Thermal resistance obtained from the results of a 3ω method for a thin insulating film with thickness of *d* on a substrate. There is an interface; The observed *R* is plotted as a function of *d*

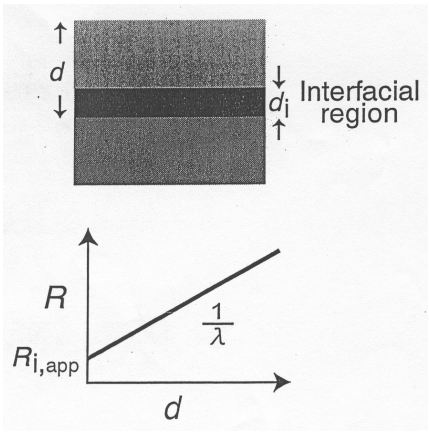

Fig. 3b Thermal resistance obtained from the results of a 3ω method for a thin insulating film with thickness of *d* on a substrate. There is an interfacial region. The observed *R* is also plotted as a function of *d*

On the other hand, if we take into account the interfacial region between the thin insulation film and the substrate as shown in the upper illustration of Fig. 3B, The observed thermal resistance is expressed as

$$R=\frac{d-d_i}{\lambda}+\frac{d_i}{\lambda_i} \tag{6}$$

where d_i is the thickness of the interfacial region and λ_i is the thermal conductivity of the interfacial region. Equation (6) is rewritten as

$$R=\frac{d}{\lambda}+R_{\mathrm{i,app}} \tag{7}$$

where

$$R_{\mathrm{i,app}}=\left(\frac{1}{\lambda_{\mathrm{i}}}-\frac{1}{\lambda}\right)d_{\mathrm{i}}. \tag{8}$$

It should be noted that Eq. (5) and Eq. (7) are essentially the same, i.e., the *d*-dependence of *R* is given by a similar function. Namely, in the lower graph of Fig. 3B, we can obtain λ, but the intercept is an apparent thermal resistance given by Eq. (8). Then, we cannot exclude the possibility of the existence of the interfacial region in the analysis of the results obtained by the 3ω method. For the interface between SiO_2 and Si, it is known that there is a strained layer with the thickness of about 1 nm, therefore it is very likely that the disordered interfacial region plays an important role in the above heat transfer.

Addendum

There are a lot of interesting subjects in the thermal characteristics of materials with a nanometer scale. They are frequently related to basic and applied advanced science and technology. Besides the subjects dealt within the present paper, there are many subjects in which the thermal characteristics in a nanometer scale should be studied. For instance, there are those for a free cluster [14], a cluster embedded in a bulk material [15], a free-standing molecular film [16], and a self-organized monolayer on a substrate [17], etc.

References

1 J. Hone, B. Batlogg, Z. Benes, A. T. Johnson and J. E. Fisher, Science, 289 (2000) 1730.
2 D. J. Fisher and P. A. Lee, Phys. Rev., B23 (1981) 6851.
3 B. J. van Wees, H. van Houten, C. W. J. Beenakker, J. G. Williamson, L. P. Kouwenhoven, D. van der Marel and C. T. Foxon, Phys. Rev. Lett., 60 (1988) 848.
4 D. Wharam, T. J. Thornton, R. Newbury, M. Pepper, H. Ahmed, J. E. F. Frost, D. G. Hasko, D. C. Peacock, D. A. Ritchie and G. A. C. Jones, J. Phys., C21 (1988) L209.
5 L. G. C. Rego and G. Kirczenow, Phys. Rev. Lett., 81 (1998) 232.
6 K. Schwab, E. A. Henriksen, J. M. Worlock and M. L. Roukes, Nature, 404 (2000) 974.
7 I. Hatta, T. Mori and F. Takahashi, Proc. of the 22nd Japan Symposium on Thermophysical Properties 2001, p.88.
8 E. T. Swartz and R. O. Pohl, Rev. Modern Phys., 61 (1989) 605.
9 I. Hatta, Y. Sasuga, R. Kato and A. Maesono, Rev. Sci. Instrum., 56 (1985) 1643.
10 T. Yao, Appl. Phys. Lett., 51 (1987) 1798.
11 I. Hatta, K. Fujii and S.-W. Kim, Mat. Sci. Eng., A292 (2000) 189.
12 S.-M. Lee and D. G. Cahill, J. Appl. Phys., 81 (1997) 2590.
13 J.-H. Kim, A. Feldman and D. Novotny, J. Appl. Phys., 86 (1999) 3959.

14 M. Schmidt, R. Kusche, W. Kronmüller, B. von Issendorff and H. Haberland, Phys. Rev. Lett., 79 (1997) 99.
15 M. Yu. Efremov, F. Schiettekatte, M. Zhang, E. A. Olson, A. T. Kwan, R. S. Berry and L. H. Allen, Phys., Rev. Lett., 85 (2000) 3560.
16 R. Geer, T. Stroebe, C. C. Huang, R. Pindak, G. Srajer, J. W. Goodby, M. Cheng, J. T. Ho and S. W. Hui, Phys. Rev. Lett., 66 (1991) 1322.
17 S. M. Clarke, A. Inaba, T. Arnold and R. K. Thomas, J. Therm. Anal. Cal., 57 (1999) 643.